Middle States Geographer; 2019, 52:14-23

AN URBAN HEAT ISLAND UNDER FLOOD CONDITIONS

D. J. Bailey
Department of Geography
Syracuse University
Syracuse, NY 13210

P. R. Baumann*
Department of Geography and Environmental Sustainability
State University of New York, College at Oneonta
Oneonta, NY 13820

ABSTRACT: *This study examines surface temperature changes within an urban area that was inundated with ponded flood water for two months. The urban area is New Orleans and the flood was created by Hurricane Katrina. The size and duration of this flood can provide a test case of what temperature conditions coastal cities might encounter in the future as water levels rise and new permanent water bodies appear around them. Using Landsat 5 thermal infrared (IR) data this study looked at surface temperatures in the New Orleans urban heat island (UHI) and adjacent wetlands for two dates, slightly before the Katrina flood and during the flood. Color composite analysis and density slicing classification were used to identify and measure temperature conditions over the study area for the two dates. Temperature maps were produced, and numerical counts of different temperature levels were ascertained. During the flood, low temperature variations existed over the flooded area in comparison to the total study area, likely creating little airflow and stagnant air.*

Keywords: *urban heat island, flooding, New Orleans, Katrina, Landsat thermal infrared*

INTRODUCTION

Global sea levels are rising. Historical tide gauge measurements indicate that a rise of 7.1 inches (18 cm) in sea levels occurred within the 100-year period between 1897 and 1997 (Douglas, 1997). More recently satellite radar measurements show that within the 24-year period from 1993 to 2017 sea levels rose by 3.0 inches (7.5 cm), a rate of about 12 inches (30 cm) per century. The current trend is expected to further accelerate during the 21st century (WCRP Global Sea Level Budget Group, 2018; Mengel, 2016). Ten percent of the world's population resides in coastal environments and two-thirds of the world's urban centers with more than 5 million people are located in these environments (McGranahan, 2007). In the United States over half of the population lives in coastal urban areas and coastal retirement communities that cover only 18 percent of the country's total land area (Klemas, 2009). With rising sea levels major urban conglomerations such as New York, Rio de Janeiro, Tokyo, and Shanghai will face increased coastal flooding that will eventually develop into new, permanent water areas and expand the size of existing water bodies. The amount of water surfaces around these urban areas will impact their development and environment (Holder, 2017).

As coastal water levels increase around these cities, urban surface temperatures are expected to increase. This study uses two different remote sensing techniques to examine land and water temperature surface conditions in the New Orleans area before and during the Katrina flood. Flood waters remained in the city for two months, and thereby, duplicated, for a short period of time, what coastal urban areas in the future might experience on a permanent basis as sea levels rise and new water bodies materialize. Two Landsat 5 Thematic Mapper (TM) data sets were used in this study. Figure 1 shows the location of the study area.

Considerable research has already been done on surface temperature conditions within UHIs (Arnfield, 2003). Also, a great amount of remote sensing imagery has been used to study the flooding and devastation of New Orleans by Katrina. However, only one major study has examined Katrina's impact on the New Orleans UHI (Lief and Lodhi, 2015). This study used thirty-two, cloud free Landsat TM data sets, extending from 1987 to 2011. Using these data sets the authors examined the loss of trees and other vegetation and how this loss impacted temperature conditions throughout the metropolitan area. The wide time period from 1987 to 2011 made it possible to include other hurricanes in the study, although Katrina was the principal storm. The primary finding from this study was that the hottest surface areas "dramatically increased" in area from 23.22 square miles (60.15km^2) in 2003 to 42.95 square miles (111.24 km^2) in 2005. The study area dealt with the urban and built-up sections of Greater New Orleans and did not include the surrounding water and wetland areas. Temperature maps based on Landsat 5's thermal

infrared data were developed. The maps used generalized temperature zone classes such as "Hottest," "Warm," and "Cooler" but did not define the numeric boundaries of the zones. In comparison the current study is directed only at the flooded areas in New Orleans and includes the wetlands, areas that are most likely to become regular water bodies as sea levels rise. Also, temperature levels or zones are numerically defined allowing for actual measurements to be ascertained.

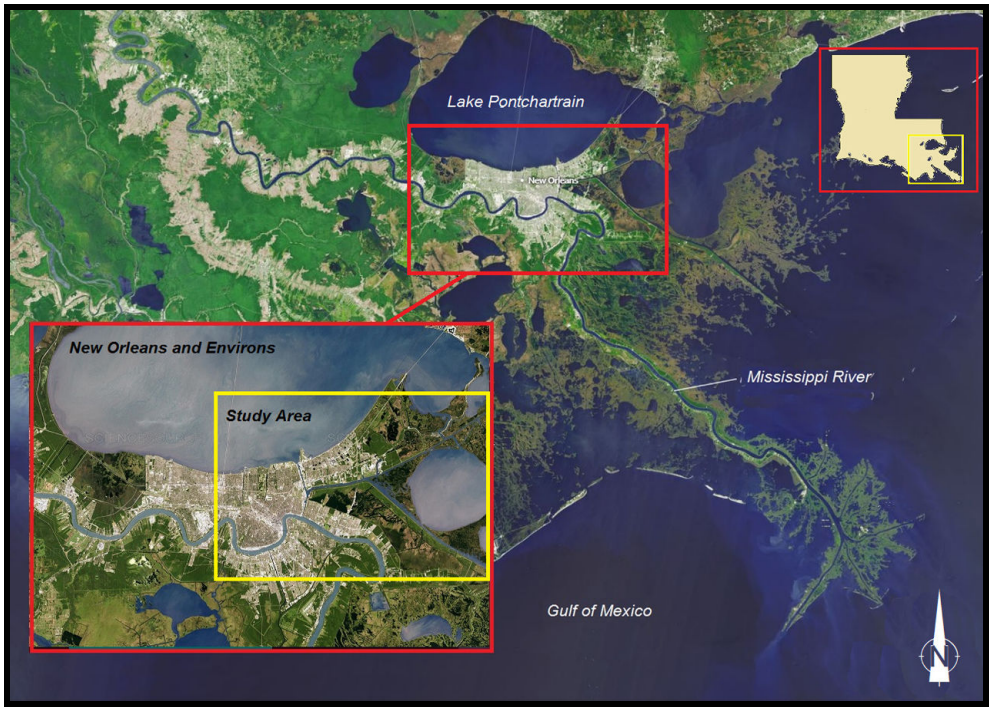

Figure 1. Study area and location.

KATRINA FLOODING

A study published by the *Journal of Hydrologic Engineering* states that "most of New Orleans proper - about 65% - is at or below mean sea level, as defined by the average elevation of Lake Pontchartrain." (Schlotzhauer, 2016) Elevations range from -13 ft (-4m) to 28 ft (8.5m). To keep the city from being inundated by water from the Lake and the Mississippi River a series of levees surround it resulting in the city having no natural means for being drained. Normal precipitation levels often cause local flooding. A network of pumping stations and canals has been built to handle such flooding with water being drained mainly into Lake Pontchartrain. This drainage system can handle 1 inch (2.5 cm) in the first hour of rainfall followed by 0.5 inch (1.3 cm) per hour thereafter. Within a period of 5 ½ to 6 hours Katrina dropped over 10 inches (25.4 cm) of rain on the city, causing flooding. The pumping stations were overwhelmed. Under these conditions the drainage system would require 19 hours to remove the rainwater from the city. However, during this period debris from the hurricane was clogging the pumping stations' grates (drains the size of 2 to 3 average size houses). Because this debris could not be removed during the storm, and for some time thereafter, some stations stopped operation to protect the pumps from being damaged. This situation led to additional flooding from the heavy rainfall (Baumann, 2006).

During the storm three major breaks in the levees-floodwalls protecting the city occurred. These breaks unleashed waves of water into the city shifting buildings off their foundations and inundating over 100,000 homes or about 35 percent of the city to varying depths up to 13 ft. (3.9m). The major breaks took place along three canals, namely the 17th Street Canal - 450 ft. (137m) breach, the London Avenue Canal/Floodwall - 300 ft. (91.4m) breach, and the Industrial Canal – 500 ft. (152.4m) breach. (Carter 2005). In addition to these three major breaks, numerous smaller breaks occurred. Two of these canals form part of the system for draining floodwater out of the city. Normally, water is pumped into these canals that drain into Lake Pontchartrain. However, as the water level in the Lake increased due to the heavy rains followed by storm surges, water was being pushed into the canals weakening

the levees and floodwalls. Residential conditions exist mainly along these canals where floodwater levels ranged between 10 and 13 ft. (3 to 3.9m) high.

IMAGERY

Two Landsat 5 Thematic Mapper (TM) satellite data sets were used in this study. These data sets were recorded around 4:20 PM on August 22, 2005 (pre-flood) and at the same time on September 7, 2005 (flood) for New Orleans and the surrounding environments. These dates relate to about a week before and a week after Katrina brought about the flooding of the city. The September image corresponds closely to the flood's fullest areal extent. The study area is frequently shrouded by clouds; thus, it is remarkable to have two cloud free days and to have them relate to when the satellite was passing over and when the Katrina flooding was occurring.

The TM system has two scanners, one that detects reflective energy in six different portions (known as bands) of the electromagnetic spectrum and one that records emitted energy in the thermal infrared portion of the spectrum. The six reflective bands have ground resolutions (pixel level) of 30m x 30m; whereas, the thermal IR band has a 120m x120m resolution. The USGS EROS (United States Geological Survey - Earth Resources Observation and Science) Center resampled the thermal IR band from a 120m to a 30m spatial resolution using the cubic convolution interpolation method. This process produced a band that corresponded spatially and geometrically with the reflective bands. All seven bands have an 8-bit radiometric resolution of 0 to 255.

The two data sets were geometrically rectified to each other and sub-data sets were created. The rectification process changed the pixel size from 30m x 30m to 28.5m x 28.5m. The sub-data sets covered the city of New Orleans and the wetlands east and the urban/wetlands south of the city, basically areas that experienced flooding (Figure 1). The sub-data sets were 1500 elements (pixels) across and 1000 lines (pixels) in size for a total of 1.5 million pixels per sub-data set. The sub-data sets covered an area of 470 square miles (1217 km^2). These sub-data sets were loaded into the image processing software package known as EarthScenes for analyses (Peet, 2004).

From the perspective of the satellite, the scanners were recording the flooded area as a combination of water, roofs of buildings, and crowns of trees. Very large portions of the flooded area had high densities of buildings and large trees, especially live oak trees. Thus, the flooded surface was neither land nor water. It was more like coastal areas that have been abandoned and surrounded by rising water levels.

WEATHER STATION DATA

Most major urban areas have only three to five official weather stations. The New Orleans Metropolitan area has five U.S. Weather Stations that collect daily maximum and minimum temperatures. Data for these five stations covering August 22 and September 7, 2005 were obtained from the National Oceanic & Atmospheric Administration (Table 1). Three of these stations were not operational during the flood period. It is difficult to compare the readings from such a small number of stations to 1.5 million recordings from a satellite. Also, the time of day when the maximum and minimum readings occurred at these weather stations is not known but the satellite temperature recordings are known. As previously indicated, they were acquired at 4:20 PM for both dates. In addition, weather stations record air temperatures, not surface temperatures. It is not possible to relate the weather station data to the satellite data, and thereby, have one data set substantiate the other data set. The weather temperature data are provided here to make readers aware of their existence, but they were not used in the study.

Table 1: Weather Station Data for New Orleans

Weather Station	Aug 22, 2005 Max.	Aug 22, 2005 Min.	Sept 7, 2005 Max.	Sept 7, 2005 Min.
Audubon Park	98°	79 °	--	--
Lakefront Airport	93°	81°	--	--
Marrero	93°	75°	--	--
New Orleans Airport	95°	74°	89°	76°
Terrytown	96°	78°	87°	74°

Source: National Oceanic & Atmospheric Administration

METHODOLOGY

Two traditional remote sensing methods namely color composite analysis and density slicing classification were used to identify and measure temperature conditions over the study area for the two dates. Before applying these methods it became necessary to determine the location and amount of water surfaces over the study area before and during the flood. This was accomplished by creating a natural color composite image with a superimposed classified near infrared image on it. This process was done for each sub-data set. Figure 2a is a natural color composite of the study area for August 22, 2005. It is based on assigning the three TM visible reflective bands, namely Band 3 (red visible with a spectral wavelength of 0.63-0.69 μm), Band 2 (green 0.52-0.60 μm), and Band 1 (blue 0.45-0.52 μm) to the RGB color guns on a monitor. After the composite was created a classified Band 4 (near infrared 0.76-0.90 μm) was superimposed on it. The near infrared is the best wavelength for separating water and land surfaces. The histogram (Figure 4c) associated with Band 4 clearly shows a dividing point between the two surfaces. Using this dividing point Band 4 was classified into two color classes. Water was assigned the color black and land the transparent white. When superimposed on the natural color composite the white allowed the land surfaces to be seen; however, the black covered the water surfaces. This process also provided a count of the number of water pixels within the study area, and thereby, made it possible to determine the amount of surface water that existed a few days before Katrina arrived. The water and land pixel counts were converted into acreage and square mile values (Table 2).

The same process was applied to the September 7, 2005 image (Figure 3a). Also, the same classification method was used with Band 4, but this time water was assigned the color red rather than black. This layer was superimposed on the natural color composite image and then the black water layer from the August image was placed on top of the red layer. The red shows the flooded areas and the black displays the normal water surfaces. Again, the process provided the total number of water pixels (Table 2). The number of water pixels in the August image is subtracted from the number of water pixels in the September image which allows the number of flooded water pixels to be determined. From this number the amount of flooded land was calculated into acres and square miles. The flooded area covered 104,371.0 acres (42,237.5 ha) or 163 sq. mi. (422 km^2) of the study area, over 7 times the size of Manhattan, NY. The number of flooded water pixels was divided by the total number of pixels in the study area resulting in the value 34.7, the percent of the total study area that was flooded.

Table 2: Preflood and Flood Counts for Total Study Area

	Preflood Image	Flood Image
Pixel Water Count	654,392	1,174,664
Pixel Land Count	845,608	325,226
Water Acreage	131,276.8 acres (53,125.8 ha)	235,647.7 acres (95,363.2 ha)
Land Acreage	169,636.2 acres (68,649.3 ha)	65,265.2 acres (26,411.9 ha)
Water Square Miles	205 sq. mi. (531 km^2)	368 sq. mi (953 km^2)
Land Square Miles	265 sq. mi. (686 km^2)	102 sq. mi. (264 km^2)

Color Composites

With the location and size of the flooded surfaces determined, the next step was to ascertain the spatial distribution of emitted energy (temperature) over the study area, especially the flooded areas. A special false color composite was developed that entailed employing Band 6 (thermal infrared 10.40-12.50μm) and the previously used Band 4, near infrared. Band 6 was assigned to the red gun on the monitor and Band 4 to both the green and blue guns (Figures 2b and 3b). As described in the section on "Imagery" Band 6 has a 120 $meter^2$ pixel resolution. This resolution was changed by USGS EROS Center to a 30 $meter^2$ pixel so that the thermal band could relate to the six reflective bands. When the seven bands were geometrically rectified Band 6 was also changed to a 28.5 $meter^2$ pixel resolution. Although the pixel size changed, Band 6's image continued to have a fuzzy appearance relative to other bands. It lacked the spatial detail of the reflective bands (Figure 4 a-Band 6 and e-Band 4).

The 8-bit radiometric scale remained the same for all seven bands and was used in constructing the histograms for the bands. The histogram (Figure 4c) for Band 6 showed that the thermal IR pixel values were tightly clustered and near the middle of the radiometric scale. This clustering partially explains why the thermal IR image (Figure 4a) lacks contrast. The image only uses a small portion of the grey levels available on an 8-bit black and white scale.

Since Band 4 (Figure 4e) was initially recorded at a higher pixel resolution than Band 6 and was designed to separate water and land, it was used in the color composite to provide spatial detail. However, with the Band 6 data values being higher on the radiometric scale than the Band 4 data values, Band 6 dominated the composite images with the red gun. The data values for the two bands needed to be in balance with each other. They were both stretched to make use of the full radiometric scale (Figure 4d). The stretching allowed two new images to be created (Figures 4b and 4f). Band 6 has more spatial detail and Band 4 more contrast. These new images were used to create Figure 2b. Figure 4 displays the process for the preflood data set. The same process was used on the flood data set (Figure 3b).

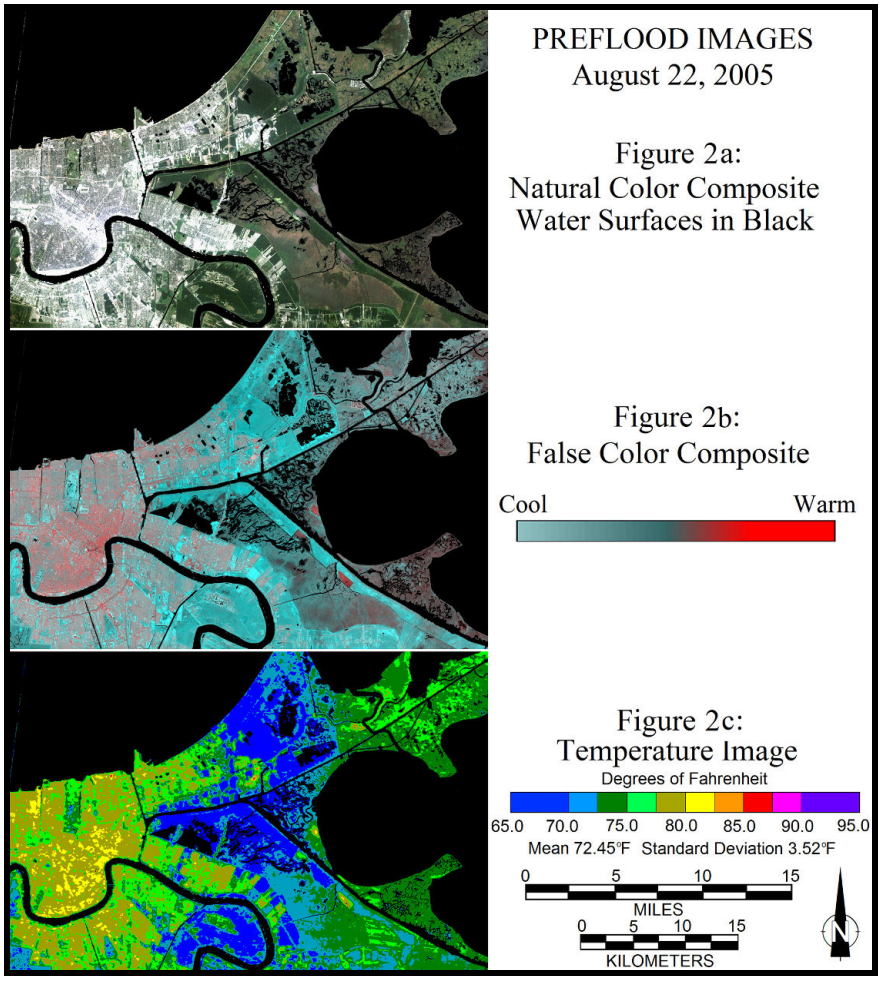

Figures 2a-c. August 22, 2005 preflood conditions.

The preflood false color composite (Figure 2b) shows high temperatures in bright red. These high temperatures are concentrated in areas with high densities of built-up urban surfaces. These areas are generally located along the Mississippi River and the shore of Lake Pontchartrain where both natural and artificial levees exist to protect property from being flooded. Moving away from the river and lake, a blending of dark red and dark blue colors can be observed indicating cooler conditions than found in the built-up areas. These colors appear in the middle of the scale for Figure 2b and relate basically to residential areas with vegetated surfaces such as lawns and trees. Outside the urban landscape a second area of blended colors exists. These areas are more dominated by the dark blue than the red colors. They are wetlands laced by water bodies. The dull red colors correspond to tall matted grass conditions. Finally, the solid bright blue areas are associated with parks and drained wetlands that are slightly elevated.

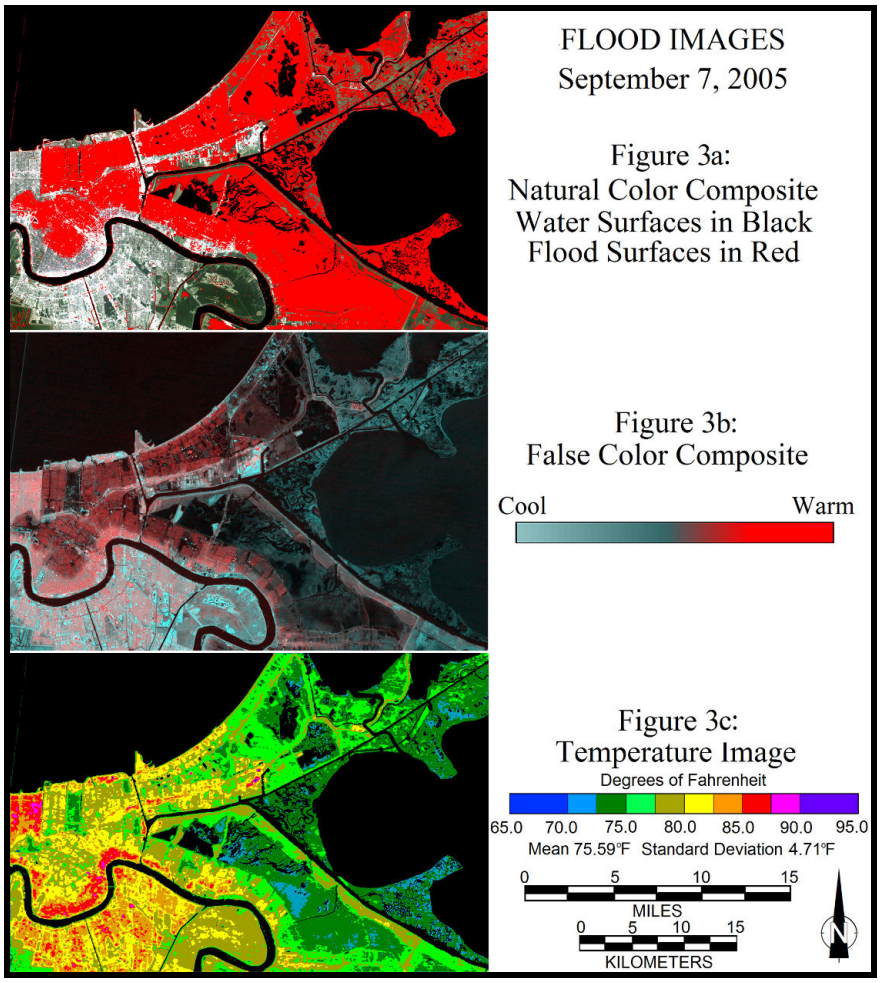

Figures 3a-c. September 7, 2005 flood conditions.

The flood false color composite (Figure 3b) shows the flooded residential areas as being dark red and the flooded parks and wetlands as being very dark blue, almost black in color. When compared to the same areas observed on Figure 2b the flooded areas on Figure 3b are warmer, especially in the wetlands. The non-flooded areas on both composites display basically the same temperature conditions with a minor increase in temperatures on Figure 3b. Thus, it appears that the flooded water created a warmer condition.

Density Slicing

The color composite images provide empirical insights into the temperature variations within the study area during the flood; however, they do not furnish any analytical data that can be used to measure the variations. The second methodology used involved employing the density slicing classification technique on Band 6 based on a regression model. A basic image associated with a spectral band consists of grey tones related to the pixel values (0 to 255). High values appear as bright grays and low values as dark grays. Density slicing divides a gray tone range into discrete classes and different colors can be assigned to each class. This process converts the image into a map, in this case a temperature map.

The National Aeronautics and Space Administration (NASA) developed a regression model that allows Landsat 5's thermal IR pixel values to be converted into temperature values (Pelta, 2016). The model's mathematical formula, as well as the temperature conversion formulas, is provided below:

Spectral Radiance = 0.1238 + 0.005632 x DN
Kelvin (ºK) = 1260.56 / (ln((607.76 / Spectral Radiance)+1))
Celsius (ºC) = ºK – 273.15
Fahrenheit (ºF) = ºC x 1.8 + 32

"DN" stands for "Digital Number" (0 to 255) and "ln" for "natural log."

The same regression model can be used for the other Landsat's that have thermal IR bands. The coefficients will be slightly different and can be found in the appropriate Landsat handbook.

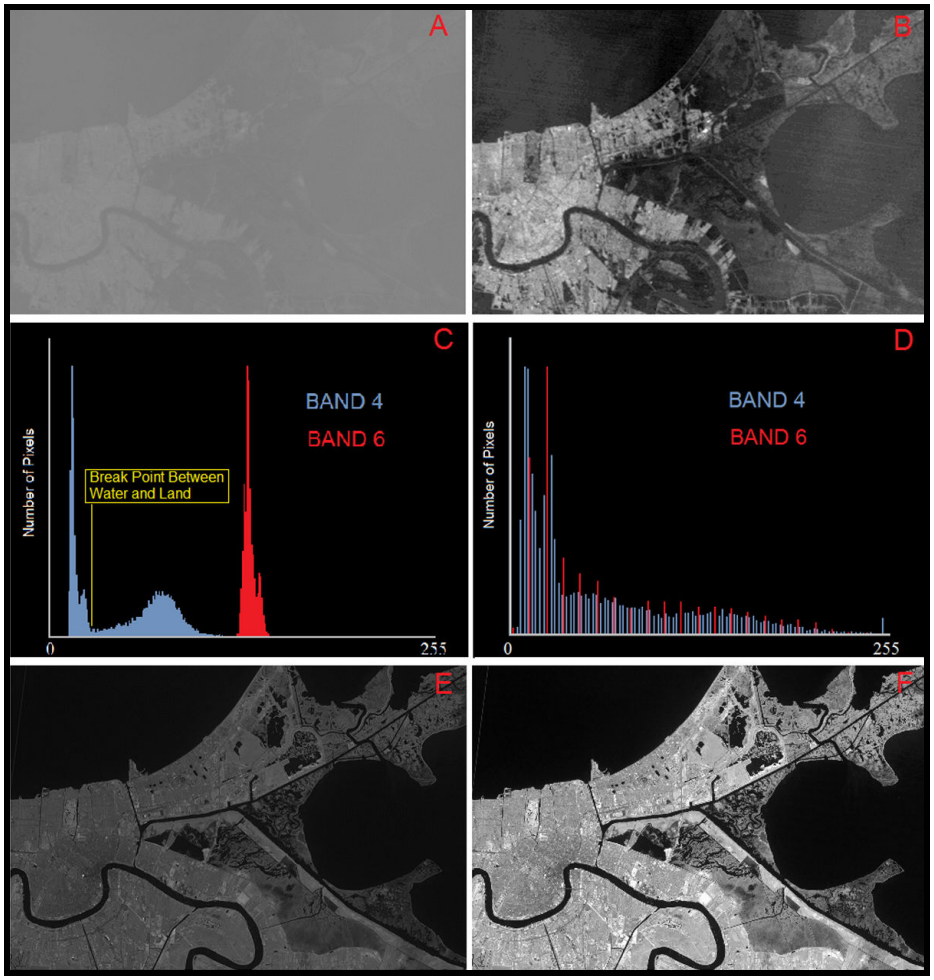

Figure 4. Preflood bands 4 and 6 pre-stretched and stretched.

The first formula is the regression model that transforms DN (Digital Number) values into spectral radiance values. The DN values have to be from the original Band 6, not a stretched or modified Band 6. The other formulas change the spectral radiance values into Kelvin temperatures followed by Celsius and Fahrenheit temperatures. Figures 2c and 3c are Fahrenheit temperature maps constructed from the thermal IR pixel values related to Band 6 for the study area's two dates. The density slicing technique was used to divide the Fahrenheit temperatures into map classes and each class was assigned a color. Regular water bodies such as Lake Pontchartrain and the Mississippi River were blacked out in order to highlight conditions over the land surface.

The group-mean temperatures for the preflood classified map, Figure 2c, and flood classified map, Figure 3c, were 72.45ºF and 75.59ºF, respectively. The group-standard deviations for the two dates were 3.53ºF and 4.71ºF. It was about three degrees warmer during the flood in comparison to the preflood date and slightly more than one-

degree standard deviation difference. These values were based on the total study area covering 1.5 million data points and included Lake Pontchartrain and other existing water bodies, as well as sizable built-up areas, that were not flooded. The preflood map displays cooler temperature conditions than the flood map. This condition is illustrated by the low temperatures over the wetland areas east and southeast of the city that appear in the blue colors. These same areas when under water are warmer.

Next, temperature conditions in only the flooded area of the total study area were examined. Figure 5a is a temperature map of the flooded area before the flood and Figure 5b during the flood. Corresponding to Figures 5a and 5b is Table 3 that provides a breakdown of the number of pixels per map class for the flooded area for the two dates. Table 3 also has the number of acres and number of square miles for each map class. These acreage figures were calculated by multiplying the number of pixels by the number of square feet (8738.51) covered by a 28.5m^2 pixel to obtain the total square feet, then dividing the square feet (43,560) per acre into the total square feet. The square mile figures were determined by dividing the number (640) of acres per square mile into the acreage amounts.

Table 3: Temperature Statistics Per Class within the Flooded Area Before and During the Flood

Map Classes (°F)	Preflood No. of Pixels	Preflood Acres	Preflood SQ. MI.	Flood No. of Pixels	Flood Acres	Flood SQ. MI.
65.0-70.0	69,627	13967.77	21.8246	13	2.60	0.0040
70.0-72.5	124,263	24928.22	38.9503	32,809	6581.76	10.2840
72.5-75.0	151,911	30474.65	47.6166	191,319	38380.23	59.9691
75.0-77.5	55,769	11187.74	17.4808	118,629	23797.99	37.1843
77.5-80.0	75,568	15159.59	23.6868	93,492	18755.29	29.3051
80.0-82.5	9,048	1815.10	2.8361	42,843	8594.67	13.4291
82.5-85.0	156	31.29	0.0488	5,341	1071.45	1.6741
85.0-87.5	21	4.21	0.0065	1,463	293.49	0.4585
87.5-90.0	4	0.80	0.0012	402	80.64	0.1260
90.0-95.0	0	0	0	56	11.23	0.0175

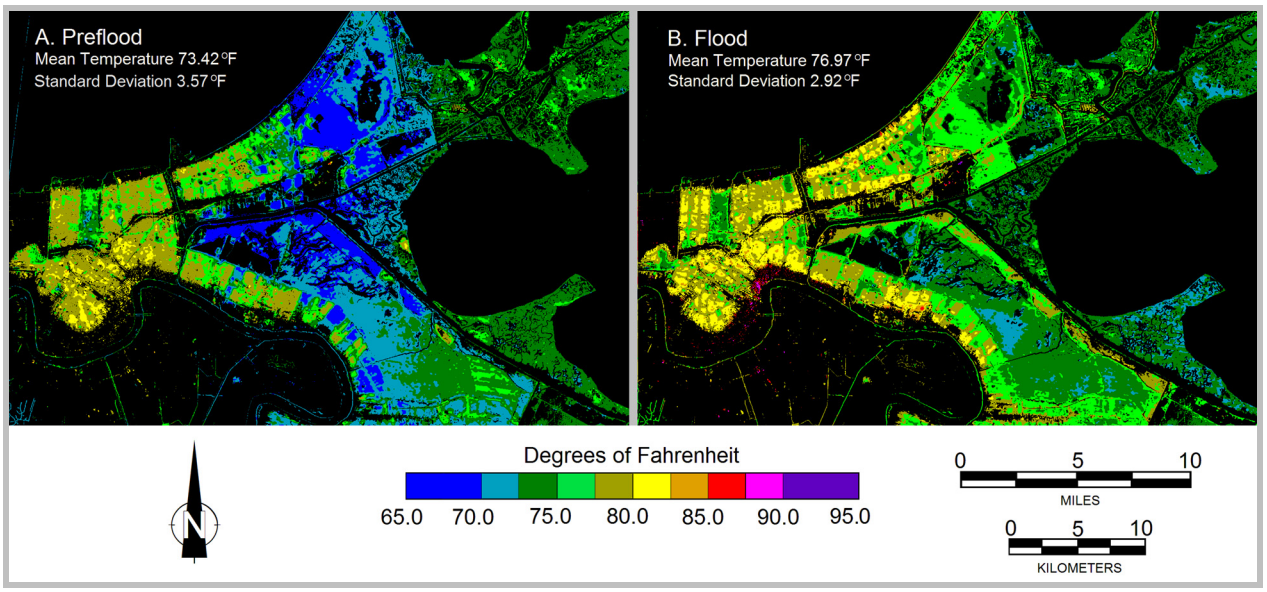

Figures 5. Temperature conditions within the flooded area before the flood and during the flood.

For the total study area, the group-mean temperatures for the preflood and flood maps, Figures 2c and 3c, were 72.45°F and 75.59°F, respectively. These mean values were previously indicated. For the flooded area the group-mean temperatures for the preflood and flood maps, Figures 5a and 5b, were 73.42°F and 75.97°F, respectively. The total number of data points for the flooded area was 486,367. These group-mean values are shown in Table 4 along with the group-standard deviation values. Even though the flood group-mean (75.59°F) for the total

study area and the flood group-mean (75.97°F) for the flooded area are almost identical their respective group-standard deviations are quite different. The group-standard deviation for the total study area on September 7 was 4.71°F and the group-standard deviation for the flooded area on the same date was 2.92°F. Temperature variations within the flooded area during the flood were less than within the total study area during the flood.

Table 4: Group-means and Group-standard Deviations

Total Study Area (1,500.000 Pixels) August 22, 2005	Total Study Area (1,500.000 Pixels) September 7, 2005	Flooded Area (486,367 Pixels) August 22, 2005	Flooded Area (486,367 Pixels) September 7, 2005
Preflood Mean = 72.45°F	Flood Mean = 75.59°F	Preflood Mean = 73.42°F	Flood Mean = 75.97°F
Preflood SD =3.52°F	Flood SD = 4.71°F	Preflood SD = 3.57°F	Flood SD = 2.92°F

CONCLUISON

This study's hypothesis was that as coastal water levels increase around cities, urban surface temperatures would increase. Comparing the group-means in the Table 4, surface temperatures for the total study area and flooded area increased 3.14°F and 2.55°F, respectively, during the flood. It could be argued that September 7 was, in general, a warmer day than August 22 but from the very limited Weather Station data available (Table 1) August 22 was the warmer of the two days.

The study also showed that based on the low group-standard deviation for the flooded area, little variation in the surface temperatures existed during the flood. This situation might relate to water surfaces generally having less temperature variation than land surfaces. The total study area has sizable land sections that were not flooded. It also has large water sections that were not part of the flooded area. Collectively these non-flooded surfaces might have played a key role in determining the high group-standard deviation for the total study area. A future study might examine the surface temperature variation over the non-flooded areas. Even though the flooded area had a low group-standard deviation, a comparison of Figures 5a and 5b shows lower surface temperature variation in the wetlands during the preflood period than the flood period. The same situation appears to occur over the built-up area. A future study might also study this situation. The low group-standard deviation also suggests that little airflow occurred over the flooded area, and thereby, the air was probably stagnant.

REFERNCES

Arnfield, A. J. 2003. Two Decades of Urban Climate Research: A Review of Turbulence, Exchanges of Energy and Water, and the Urban Heat Island. *International Journal of Climatology* 23 (1): 1-26. https://rmets.onlinelibrary.wiley.com/doi/abs/10.1002/joc.859 (last access Jan. 2019)

Baumann P.R., W. A Mitteager, and M. D. Nellis. 2006, Katrina: The 'Big One' Arrived *Geocarto International* 21 (2): 75-80.

Douglas, B. C. 1997. Global Sea Rise: A Redetermination. *Surveys in Geophysics* 18 (2/3): 279–292. https://link.springer.com/article/10.1023/A:1006544227856

Holder J., N. Kommenda, and J. Watts. 2017. The UN is warning that we are now on course for 3C of global warming. This will ultimately redraw the map of the world. *The Guardian.* ISSN 0261-3077. (last access Dec. 28, 2018).

Intergovernmental Panel on Climate Change (IPCC). 2018: Global Warming of 1.5°C.An IPCC Special Report on the impacts of global warming of 1.5°C above pre-industrial levels and related global greenhouse gas emission pathways, in the context of strengthening the global response to the threat of climate change, sustainable development, and efforts to eradicate poverty. *World Meteorological Organization, United Nations Environment Programme* https://www.ipcc.ch/sr15/download/

Klemas, V.V. 2009. The Role of Remote Sensing in Predicting and Determining Coastal Storm Impacts. *Journal of Coastal Research* 25 (6): 1264 – 1275.

Lief, A.P and A.L Mahtab. 2015. The impact of Hurricane Katrina on the New Orleans urban heat island. *Anais XVII Simpósio Brasileiro de Sensoriamento Remoto* João Pessoa, Brazil April 25-29: 4519-4526.

McGranahan, G., D. Balk, and B. Anderson. 2007. The rising tide: assessing the risks of climate change and human settlement in low elevation coastal zones. *Environment and Urbanization* 19 (1): 17-37. https://doi.org/10.1177/0956247807076960

Mengel, M., A. Levermann, K. Frieler, A. Robinson, B. Marzeion, and R. Winkelmann . 2016. Future sea level rise constrained by observations and long-term commitment. *Proceedings of the National Academy of Sciences.* 113 (10): 2597–2602.

Pelta R., A.Chudnovsky, and J. Schwartz. 2016. Spatio-temporal behavior of brightness temperature in Tel-Aviv and its application to air temperature monitoring**.** *Environmental Pollution* **,** 208 (Part A): 153-160. https://www.sciencedirect.com/science/article/pii/S0269749115300531?via%3Dihub (last access May. 2020).

Peet, F. 2004. EarthScenes, Version2.4 [Computer Software]. Eidetic Digital Imaging Ltd. Brentwood Bay, British Columbia, Canada.

Schlotzhauer, D. and W. S. Lincoln. 2016. Using New Orleans Pumping Data to Reconcile Gauge Observations of Isolated Extreme Rainfall due to Hurricane Isaac. *Journal of Hydrologic Engineering*, 21 (9): 1943-5584 https://ascelibrary.org/doi/abs/10.1061/(ASCE)HE.1943-5584.0001338 (last access Jan. 2019).

WCRP Global Sea Level Budget Group, 2018. Global sea-level budget 1993–present. *Earth System Science Data*. **10** (3): 1551–1590. https://doi.org/10.5194/essd-10-1551-2018